Experimental Study of Lithium-ion Battery Thermal Behaviour Under Abuse Discharge Condition

Open Access

Zul Hilmi Che Daud[1,*], Zainab Asus[1], Izhari Izmi Mazali[1], Mohd Kameil Abdul Hamid[1], Adam Maxwell Doumin[1], Fitri Yakub[2]

[1] School of Mechanical Engineering, Faculty of Engineering, Universiti Teknologi Malaysia, 81310 Skudai, Johor, Malaysia
[2] Malaysia-Japan International Institute of Technology, Universiti Teknologi Malaysia, 54100, Kuala Lumpur, Malaysia

ARTICLE INFO

ABSTRACT

This article presents the impact of abuse discharge condition on the battery cell surface temperature. The abuse discharge condition is when the battery is discharge down to 10% State of Charge (SOC). To determine the temperature evolution of the battery cell surface, a series of experiments is conducted. Three battery cells in a battery pack are discharged at 1C, 3C, and 5C discharge rate with a constant cooling air velocity of 2 m/s. The battery is discharge from 100% SOC down to 10% SOC to simulate the abuse discharge condition. Experimental results show that discharging the battery at SOC lower than 20% contributes to a radical increase of cell temperature at all battery cell locations impacted by a sudden increase of internal resistance's value in this region.

1. Introduction

The problem of shortage of the crude oil for energy supply due to the increase of demand without the expansion of oil production [1] and the environment pollution urgently require the development and utilization of alternative powertrain [2]. Hybrid Electric vehicle (HEVs) is a good alternative choice over conventional powertrain architecture due to better fuel efficiency and other environmental benefits [3]. Lithium ion battery is one of the preferred power sources in hybrid electric vehicles (HEVs) application because of higher energy density, power density and no memory effect compared to other type of batteries. Lithium ion battery offers fast acceleration capability and long driving range that makes them very suitable for HEVs applications [3].

Temperature is one of the parameters of a lithium ion battery that has to be carefully controlled, because the battery's working temperature greatly influences efficiency, cell degradation, and the battery's life time [4]. The temperature of each cell inside the battery pack varies, depending on the battery pack's design. Temperature variations may lead to over-charge or over-discharge during

---

* *Corresponding author.*
E-mail address: hilmi@mail.fkm.utm.my (Zul Hilmi Che Daud)

cycling which further contribute to premature failure in the battery packs in the form of accelerating capacity fading or thermal runaway [5,6].

Various experimental works regarding battery cell surface temperature can be found in literature. These works can be divided into several groups, depending on the methods used in temperature measurement, number of cells, charge/discharge methods, and type of cooling system used. Some works only consider a homogeneous temperature [7-9], but most recent works consider non homogeneous temperature throughout the cell surface [10-16]. For non-homogeneous temperature, normally, cell temperature near the positive and negative terminal is higher than in other locations, with temperature differences varying from one work to another. The number of cells used in experiment can vary from a single cell to several cells combined in a battery pack.

The experimental works that put into evidence the cell temperature evolution at all cell locations for a single cell as well as the impact of packaging several cells in a battery pack, using different discharge rates and different cooling air velocities as cooling system is discussed in [17]. However, it is found that most of the existing works only discuss the cell temperature at a relatively high SOC. Methods for estimating the value of SOC are discussed in [18]. There are still lacks of results that show what happens to the battery cell thermal behaviour when the cell is discharged to small SOC, less than 20%. This study highlights the battery cell temperature behavior under abuse discharge condition (discharge at SOC less than 20%) and impact of different SOC on the battery cell internal resistance.

2. Methodology
2.1 Experimental Set-up

Experiment is conducted for three lithium-ion battery cells placed inside a battery box. The cells are connected in series electrically and arranged in parallel inside a battery box, as shown in Figure 1. The battery used is a Lithium ion battery from Kokam SLPB 100216216H cells that have a typical capacity of 40 Ah. The maximum current allowed is 200 A during discharge and 80 A during charge. Each cell has a weight of 1.1 kg measuring 10 mm thickness, 215 mm width, and 210 mm length. Each cell has a nominal voltage of 3.7 V. The choice of this type of cell is based on the consideration that the cell's specifications are suitable to be used in both Electric Vehicles (EVs) and Hybrid Electric Vehicles (HEVs).

In Figure 1, the arrow indicates air flow direction. An 18 mm space between each cell enables air to circulate and create a forced convection cooling system that takes heat from the cell surface into the surrounding environment. Figure 2 shows the battery cells in the box with thermocouples attached to the cell surfaces. The thermocouples are attached to the cell surfaces thank to auto-adhesive head of 25x19 mm. The wires of the thermocouples with a diameter of 2 mm are arranged in a way to minimize their influence on the movement of the cooling air.

Three cell surfaces are chosen to be monitored, marked as 1R, 1L, and 2R as indicate in Figure 1. Surface 1R and 1L are for the first cell on the right and left side of the cell respectively, while 2R is at the right side of the second cell. Eight thermocouples are placed on each monitored cell surface at various locations as shown in Figure 3. In general, three thermocouples are placed at 30 mm from top edge of the cell near the positive and negative electrode terminal, three in the middle of the cell, and two at 30 mm from bottom edge of the cell. This arrangement is important in order to capture the cell surface temperature for the whole surface area with minimum amount of thermocouples used. A total of 24 thermocouples are used for the three surfaces. The thermocouples at different positions of the cell surface are marked by P1 to P24, see Figure 3. Thermocouple P1-P8 and P9-P16

are on the first cell at surface 1R and 1L respectively, while P17-P24 are on the second cell at surface 2R. The arrow indicates air flow direction.
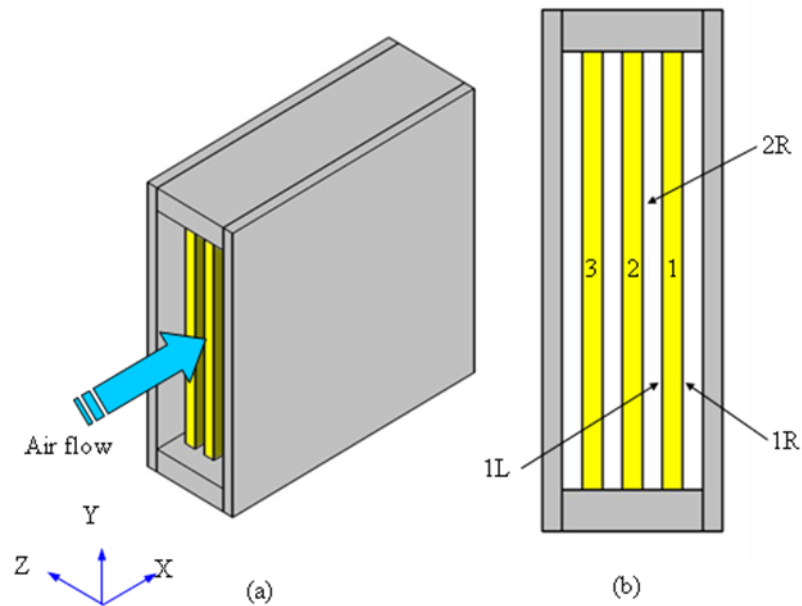
Fig. 1. Battery cells arrangement in the box with (a) represent the isometric view and (b) the front view
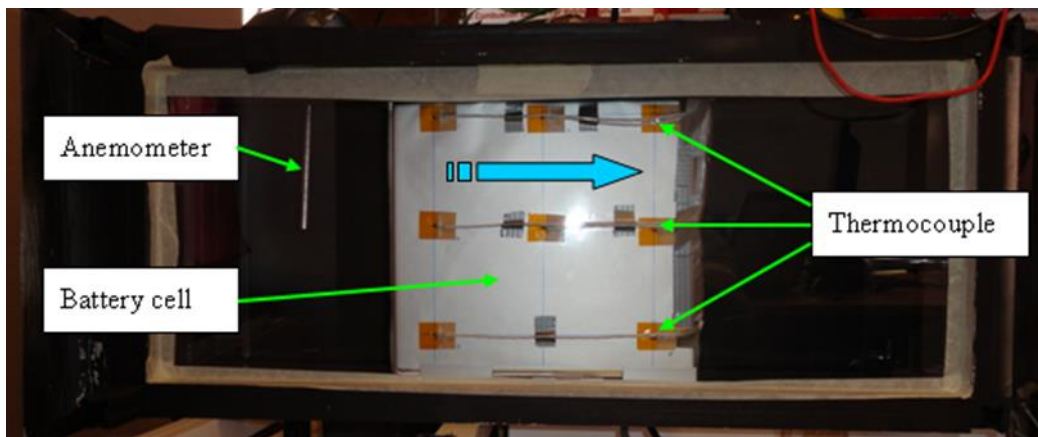
Fig. 2. Battery cells in the box with thermocouples and anemometer
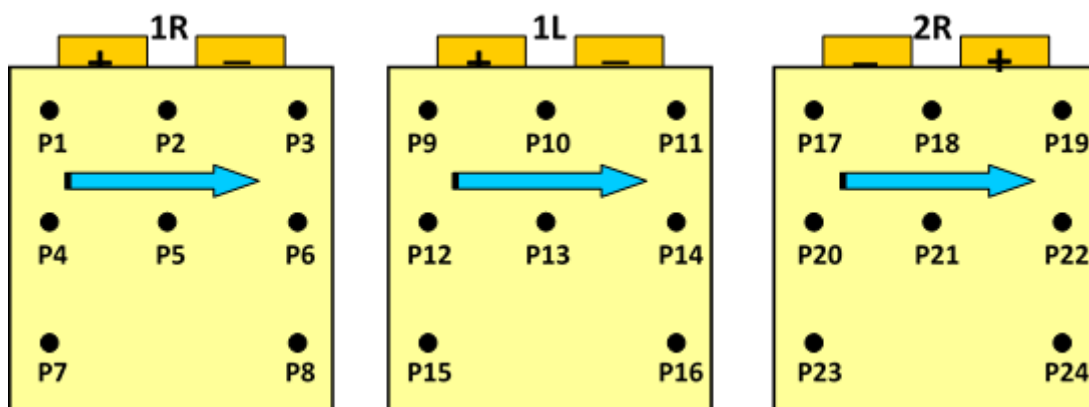
Fig. 3. Position of thermocouples and air flow direction at surface 1R, 1L, and 2R

2.2 Experimental procedure

To determine the temperature evolution of the battery cell surface, a series of experiments is conducted with different discharge rates and cooling air velocities. The battery is discharged at 1C (40 Amps), 3C (120 Amps), and 5C (200 Amps) discharge rate from 100% SOC to 10% SOC with a constant cooling air velocity of 2 m/s, 4 m/s, 6 m/s, 8 m/s and 10 m/s (This article will focus on 2 m/s only). The cooling air temperature is at room temperature, which happens to be on 22°C during experiments. The experimental procedure is as follows:

I.   The experiment is conducted only when the battery cells are full charge. It is considered that the battery cells are fully charged or 100 % SOC when the battery total voltage is equal to 12 Volts or 4 Volts per cell.
II. The charging process is stopped one hour before starting the experiment and the cells are left to cool down naturally to make sure that the temperature increase during charging does not affect the temperature measurement during discharge.
III. Example here is for 1C discharge rate at cooling air velocity of 2 m/s.
IV. The experiment is started by setting the fan speed in order to obtain the desired constant cooling air velocity, 2 m/s.
V.   At this stage the essential information is recorded; air velocity, air temperature, and battery cell voltage.
VI. The battery cells are then discharged at a constant discharge rate, 1C discharge rate (40 Amps).
VII. The discharge process is continued until the battery SOC reaches a limit of 10% SOC. The battery cell SOC is calculated using battery model as stated in [19,20].
VIII. The cooling air velocity is maintained constant at 2 m/s from t=0s until 100 seconds after the end of discharge process, in order to reduce the battery cell temperature rapidly after the end of discharge.
IX. During discharge process, several parameters are monitored to ensure the validity of experiment result and for safety reasons. These include the constant cooling air velocity at 2 m/s, cooling air temperature, maximum cell surface temperature which has to stay below 60°C, and the battery voltage above 2.7 Volts.
X.   The experimental results including cell temperatures, battery voltage and current and cooling air velocity and temperature are recorded automatically through Labview software at the frequency of 10 Hz.

The experimental procedure is than repeated for 3C and 5C discharge rate at air velocity of 2 m/s, 4 m/s, 6 m/s, 8 m/s, and 10 m/s. This article will focus on the thermal behavior on abuse condition. So, the temperature at P1, P5, and P7 on first cell and P19, P21, and P23 on second cell with cooling air velocity of 2 m/s will be discussed in detailed. The distribution of temperature at other locations as well as effect of cooling system is discussed in [21].

3. Results

Figure 4-Figure 6 show the temperature evolution of the first cell (surface 1R) at P1, P5, and P7 for 1C, 3C, and 5C discharge rate respectively. Figure 7-Figure 9 show the temperature evolution of the second cell (surface 2R) at P19, P21, and P23 for 1C, 3C, and 5C discharge rate respectively. Separator "I" indicates the discharge time at 20% SOC and separator "II" is the end of discharge at

10% SOC. In general, the cell surface temperatures increase steadily at the beginning of discharge until 20% SOC for all three discharge rates. After 20% SOC until the end of discharge, there is a sudden increase of temperature for all 6 locations. This phenomenon is explained by Lin *et al.,* [4] by the huge increase of the value of internal resistance between 20% SOC and 10% SOC. This is one of the reasons why it is dangerous to discharge the battery to less than 20% SOC. The description and different values of internal resistance as a function of SOC can also be found in [17,19].
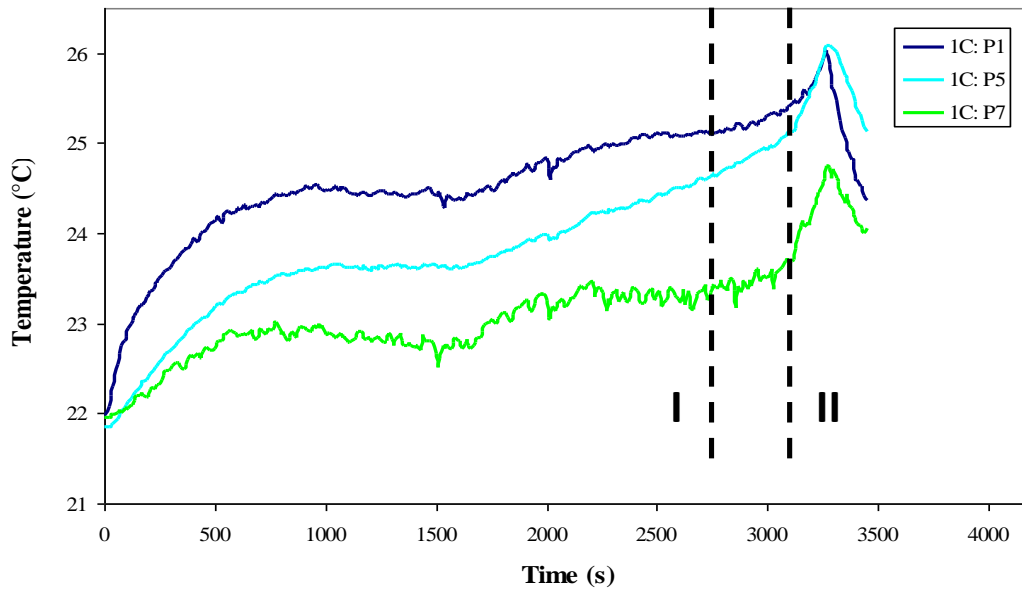
Fig. 4. Cell surface temperature evolution under 1C discharge rate at cooling air velocity of 2 m/s for abuse discharge at first cell
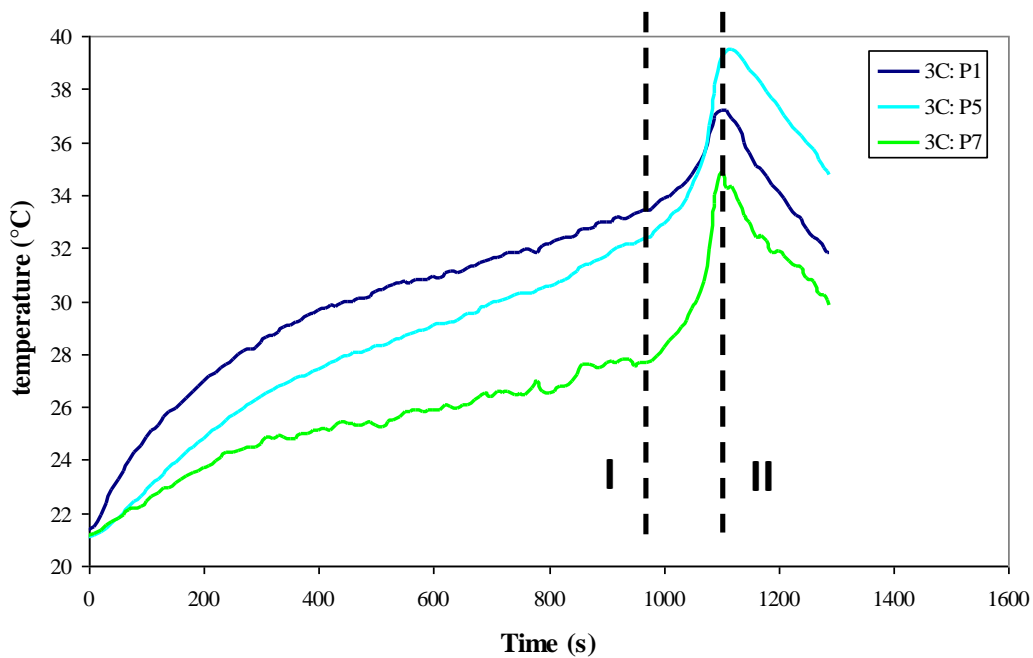
Fig. 5. Cell surface temperature evolution under 3C discharge rate at cooling air velocity of 2 m/s for abuse discharge at first cell
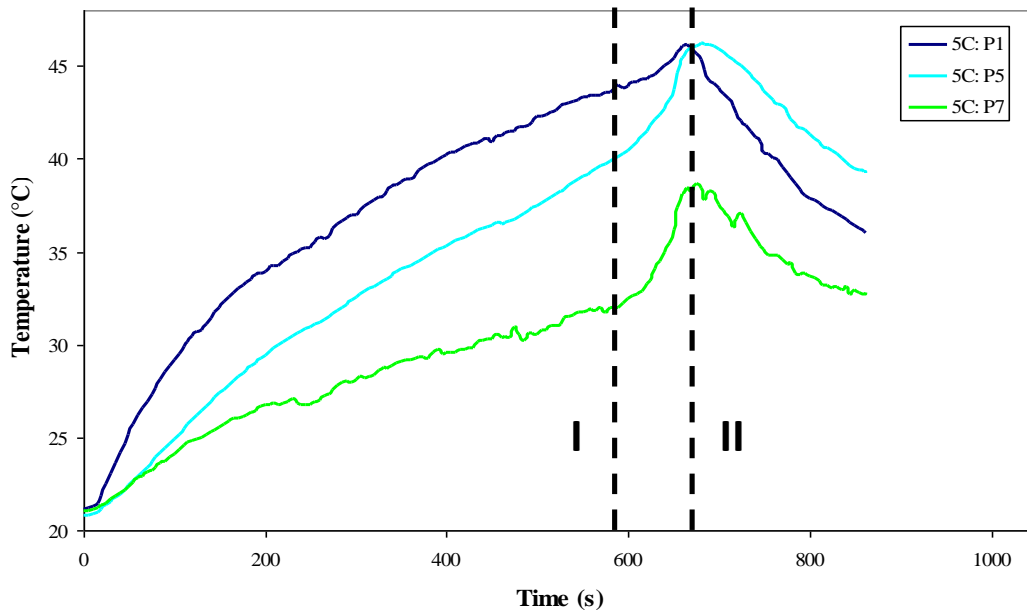
Fig. 6. Cell surface temperature evolution under 5C discharge rate at cooling air velocity of 2 m/s for abuse discharge at first cell
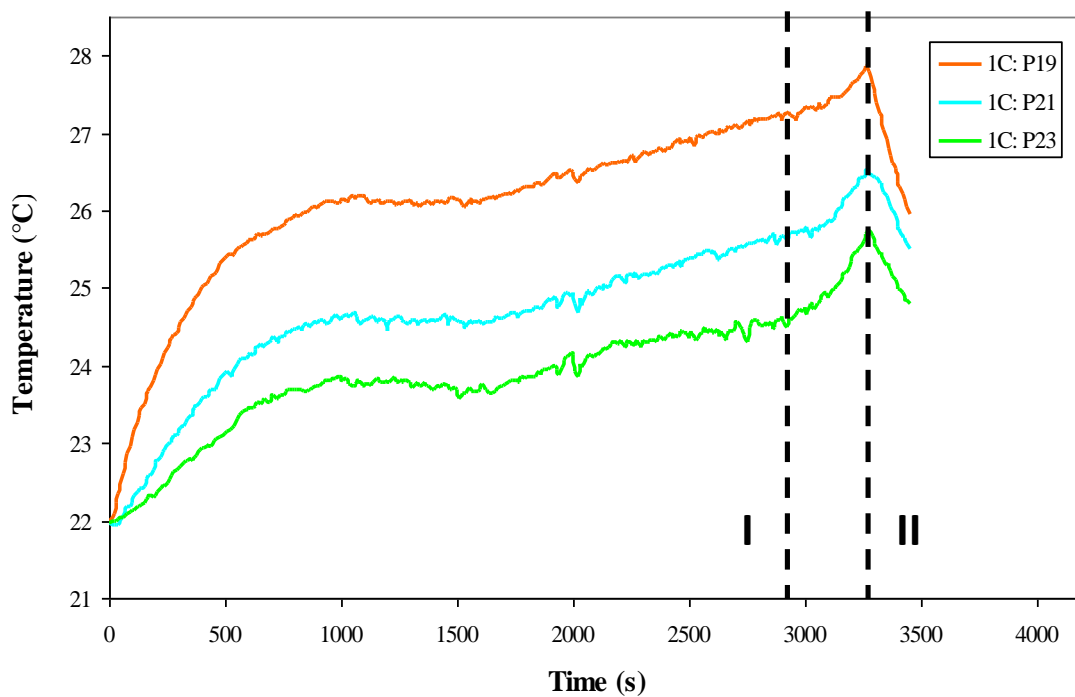
Fig. 7. Cell surface temperature evolution under 1C discharge rate at cooling air velocity of 2 m/s for abuse discharge at second cell

Penerbit
Akademia Baru
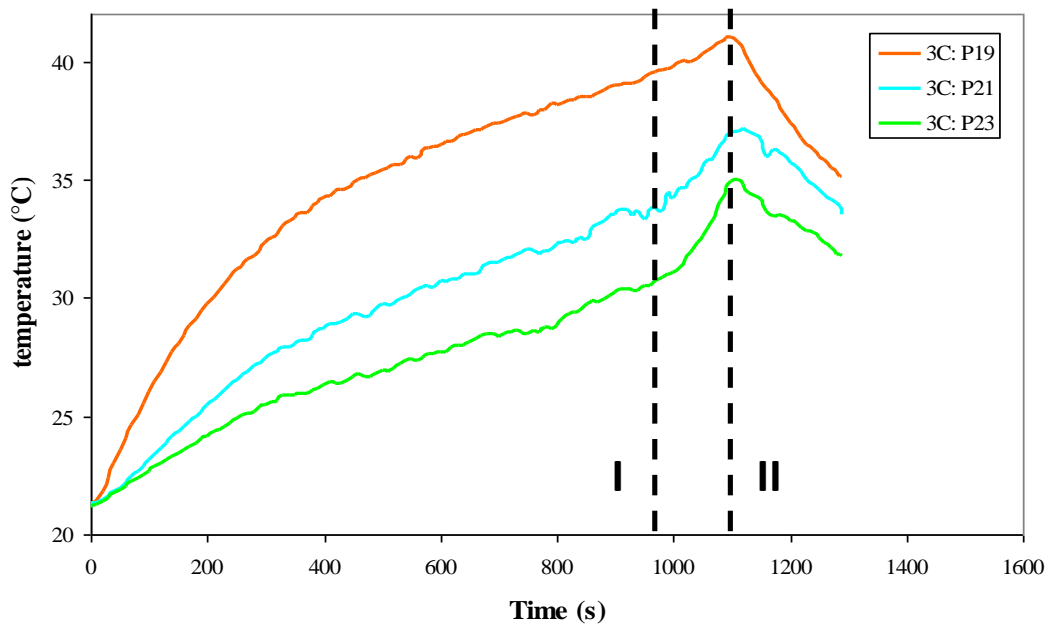
Fig. 8. Cell surface temperature evolution under 3C discharge rate at cooling air velocity of 2 m/s for abuse discharge at second cell
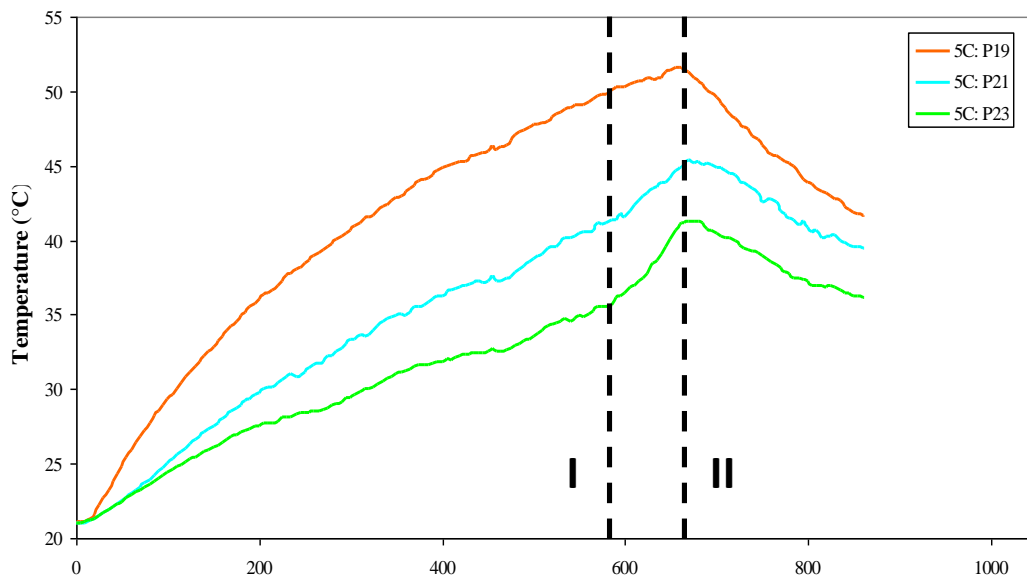
Fig. 9. Cell surface temperature evolution under 5C discharge rate at cooling air velocity of 2 m/s for abuse discharge at second cell

3.1 First Cell at Different Discharge Rates

In general, the temperature evolution at 20% SOC to 10% SOC is similar for all three discharge rates (1C, 3C and 5C) with two distinctive temperatures recorded; one higher temperature for P1, and P5, and one lower temperature for P7. At 1C discharge rate, the temperature increases to only two distinctive temperatures, 26°C for P1 and P5, and 24.5°C for P7, even though temperature for all locations are different at 20% SOC. At 10% SOC, P1 is no longer the hottest location. There is no more effect of high current densities at negative and positive electrodes and also the difference of the electrical conductivity on the temperature increases. At 3C the value of temperature increase is 4°C at P1 and 6.0°C at P5 and P7. Finally, at 5C discharge rate, between 20% SOC to 10% SOC, temperature differences is around 3°C at P1 and 6°C at P5 and P7. The value of temperatures at the end of discharge at 10% SOC and their differences with the temperature at 20% SOC are listed in Table 1.

For all three discharge rates, the smallest temperature increase is at P1 and the biggest temperature increase is observed at P7. This means that location near the positive electrode will have less temperature increase than other part of battery cell while temperature for location far from positive electrode will increase the most. At 1C discharge rate, temperature from 20% SOC to 10% SOC increase from 3-6%, 11-22% for 3C discharge, and 6-20% for 5C discharge.

Table 1
The values of Reynolds number and velocity

Discharge rate	Temperature (°C)	P1	P5	P7
1C	At 20% SOC	25.2	24.8	23.3
	At 10% SOC	25.9	25.9	24.6
	Difference	0.7	1.1	1.2
	% increase	2.9	4.6	5.2
3C	At 20% SOC	33.3	32.3	27.7
	At 10% SOC	36.8	37.8	33.7
	Difference	3.5	5.6	6.0
	% increase	10.6	17.2	21.7
5C	At 20% SOC	43.5	39.7	31.7
	At 10% SOC	46.1	45.5	38.1
	Difference	2.5	5.8	6.4
	% increase	5.8	14.6	20.1

3.2 Second Cell at Different Discharge Rates

In general, the temperature increases gradually from 100% SOC to 20% SOC for all three discharge rates (1C, 3C and 5C). Temperature at P19 is the highest for all three discharge rates followed by P21 and P23. From 20% SOC to 10% SOC, the temperature increases at higher rate compared to the

temperature increases from 100% SOC to 20% SOC. Anyhow, the temperature increases from 20% SOC to 10% SOC at second cell is lower than at the first cell. The temperature increases from 20% SOC to 10% SOC is between 0.2°C to 1.1°C at 1C discharge, 1.3°C to 4.1°C at 3C discharge and 1.4°C to 5.8°C at 5C discharge. For all three discharge rates, the highest temperature at 10% SOC is at P19 while the lowest temperature is recorded at P23. The value of temperatures at the end of discharge at 10% SOC and their differences with the temperature at 20% SOC are listed in Table 2.

Since the increase of temperature at abuse condition is much affected by the increase of battery internal resistance at low SOC, the experimental result of the battery internal resistance at different SOC is presented. Experiment is conducted with 0.5°C step discharge current, at 22°C. Throughout the experiment, cooling air at adapted velocity may be used in order to keep the battery cell temperature constant at 22°C. Experimental procedure follows several steps. Figure 10 shows the battery internal resistance as a function of SOC at 22°C. It shows that the resistance is nearly constant at the range 100% to 20% SOC. In this range, the value of internal resistance varies between 1.8-2.17 mΩ. After 20% SOC, there is a sudden jump in the value of internal resistance. At 5 % SOC the value of internal resistance is 3.7 mΩ, which is almost two times the initial value at 100% SOC. These analyses confirm the observation in [4,22].

Table 2
Temperature at end of discharge for 20% SOC and 10% SOC at air velocity of 2m/s for second cell (surface 2R)

Discharge rate	Temperature (°C)	P19	P21	P23
1C	At 20% SOC	27.2	25.6	24.6
	At 10% SOC	27.8	26.4	25.6
	Difference	0.6	0.9	1.0
	% increase	2.1	3.4	4.1
3C	At 20% SOC	39.5	33.7	30.5
	At 10% SOC	41.0	36.7	34.4
	Difference	1.5	3.0	3.9
	% increase	3.7	9.0	12.8
5C	At 20% SOC	49.8	41.1	35.6
	At 10% SOC	51.6	44.9	41.2
	Difference	1.8	3.8	5.6
	% increase	3.6	9.2	15.7
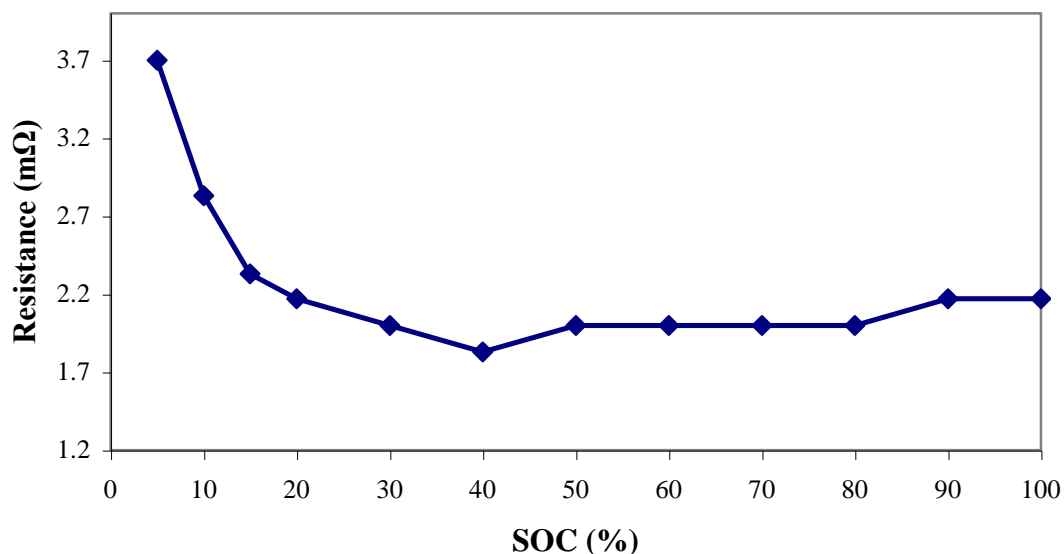
Fig. 10. Battery resistance as a function of SOC

4. Conclusions

Discharging the battery at SOC lower than 20% reveals a sudden huge increase of cell temperature at all battery cell locations. This situation is directly influenced by the change of the value of internal resistance at different SOC. Experiments show that at a constant temperature, the variation of internal resistance is small from 100% to 20% SOC. Anyhow, after 20% SOC there is a sudden jump in the value of internal resistance. This explains why it is dangerous to discharge the battery to less than 20% SOC.

Acknowledgement

References
[1] Khattak, Muhammad Adil, Mohammad Azfar Haziq Ayoub, Muhammad Ariff Fadhlillah Abdul, Mohd Faidhi Mahrul Manaf, Mohd Ridwan Mohd Juhari, Mira Idora Mustaffa, and Suhail Kazi. "Global Energy Security and European Union: A Review."

[2] Liu, Feifei, Fengchong Lan, and Jiqing Chen. "Dynamic thermal characteristics of heat pipe via segmented thermal resistance model for electric vehicle battery cooling." *Journal of Power Sources* 321 (2016): 57-70.

[3] Kwon, Hyukjoon, Michael Sprengel, and Monika Ivantysynova. "Thermal modeling of a hydraulic hybrid vehicle transmission based on thermodynamic analysis." *Energy* 116 (2016): 650-660.

[4] Shafiei, Arash, Ahmadreza Momeni, and Sheldon S. Williamson. "Battery modeling approaches and management techniques for plug-in hybrid electric vehicles." In *Vehicle Power and Propulsion Conference (VPPC), 2011 IEEE*, pp. 1-5. IEEE, 2011.

[5] Abdul-Quadir, Yasir, Perttu Heikkilä, Teemu Lehmuspelto, Juha Karppinen, Tomi Laurila, and Mervi Paulasto-Kröckel. "Thermal investigation of a battery module for work machines." In *Thermal, Mechanical and Multi-Physics Simulation and Experiments in Microelectronics and Microsystems (EuroSimE), 2011 12th International Conference on*, pp. 1-6. IEEE, 2011.

[6] Al-Hallaj, Said, and J. Robert Selman. "Thermal modeling of secondary lithium batteries for electric vehicle/hybrid electric vehicle applications." *Journal of power sources* 110, no. 2 (2002): 341-348.

[7] C. Lin, K. Chen, F. Sun, P. Tang, and H. Zhao. "Research on thermo-physical properties identification and thermal analysis of EV li-ion battery." *Vehicle Power and Propulsion Conference (VPPC)*, pages 1643–1648, Dearborn, September 7-11 2009.

[8] Rad, M. Shadman, D. L. Danilov, M. Baghalha, M. Kazemeini, and P. H. L. Notten. "Adaptive thermal modeling of Li-ion batteries." *Electrochimica acta* 102 (2013): 183-195.

[9] Watrin, Nicolas, Robin Roche, Hugues Ostermann, Benjamin Blunier, and Abdellatif Miraoui. "Multiphysical lithium-based battery model for use in state-of-charge determination." *IEEE Transactions on Vehicular Technology* 61, no. 8 (2012): 3420-3429.

[10] Chacko, Salvio, and Yongmann M. Chung. "Thermal modelling of Li-ion polymer battery for electric vehicle drive cycles." *Journal of Power Sources* 213 (2012): 296-303.

[11] Kim, Ui Seong, Jaeshin Yi, Chee Burm Shin, Taeyoung Han, and Seongyong Park. "Modelling the thermal behaviour of a lithium-ion battery during charge." *Journal of Power Sources* 196, no. 11 (2011): 5115-5121.

[12] Awarke, Ali, Martin Jaeger, Oezen Oezdemir, and Stefan Pischinger. "Thermal analysis of a Li-ion battery module under realistic EV operating conditions." *International Journal of Energy Research* 37, no. 6 (2013): 617-630.

[13] Giuliano, Michael R., Suresh G. Advani, and Ajay K. Prasad. "Thermal analysis and management of lithium–titanate batteries." *Journal of Power Sources* 196, no. 15 (2011): 6517-6524.

[14] Kim, Ui Seong, Chee Burm Shin, and Chi-Su Kim. "Effect of electrode configuration on the thermal behavior of a lithium-polymer battery." *Journal of Power Sources* 180, no. 2 (2008): 909-916.

[15] Kim, Ui Seong, Chee Burm Shin, and Chi-Su Kim. "Modeling for the scale-up of a lithium-ion polymer battery." *Journal of Power Sources* 189, no. 1 (2009): 841-846.

[16] Pesaran, Ahmad A., and Matthew Keyser. "Thermal characteristics of selected EV and HEV batteries." In *Proceedings of the Annual Battery Conference: Advances and Applications, Long Beach, CA, Jan*, pp. 9-12. 2001..

[17] Daud, Zul Hilmi Che, Daniela Chrenko, El-Hassane Aglzim, Alan Keromnes, and Luis Le Moyne. "Experimental Study of Lithium-Ion Battery Thermal Behaviour for Electric and Hybrid Electric Vehicles." In *Vehicle Power and Propulsion Conference (VPPC), 2014 IEEE*, pp. 1-6. IEEE, 2014.

[18] Omairi, Amzar, and Z. H. Ismail. "Modeling battery state of charge in wireless sensor networks based on structured multi-layer perceptron." *Journal of Advanced Research in Applied Sciences and Engineering Technology* 5, no. 2 (2016): 36-45.

[19] Chen, Min, and Gabriel A. Rincon-Mora. "Accurate electrical battery model capable of predicting runtime and IV performance." *IEEE transactions on energy conversion* 21, no. 2 (2006): 504-511.

[20] Erdinc, Ozan, Bulent Vural, and Mehmet Uzunoglu. "A dynamic lithium-ion battery model considering the effects of temperature and capacity fading." In *Clean Electrical Power, 2009 International Conference on*, pp. 383-386. IEEE, 2009.

[21] Sun, Fengchun, Rui Xiong, Hongwen He, Weiqing Li, and Johan Eric Emmanuel Aussems. "Model-based dynamic multi-parameter method for peak power estimation of lithium–ion batteries." *Applied Energy* 96 (2012): 378-386.

[22] Baronti, F., G. Fantechi, E. Leonardi, R. Roncella, and R. Saletti. "Enhanced model for lithium-polymer cells including temperature effects." In *IECON 2010-36th Annual Conference on IEEE Industrial Electronics Society*, pp. 2329-2333. IEEE, 2010.